

Is a convergently derived muscle-activity pattern driving novel raking behaviours in teleost fishes?

Nicolai Konow* and Christopher P. J. Sanford

Department of Biology, 114 Hofstra University, Hempstead, NY 11549, USA

*Author for correspondence (e-mail: nicolai.konow@hofstra.edu)

Accepted 14 January 2008

SUMMARY

Behavioural differences across prey-capture and processing mechanisms may be governed by coupled or uncoupled feeding systems. Osteoglossomorph and salmonid fishes process prey in a convergently evolved tongue-bite apparatus (TBA), which is musculoskeletally coupled with the primary oral jaws. Altered muscle-activity patterns (MAPs) in these coupled jaw systems could be associated with the independent origin of a novel raking behaviour in these unrelated lineages. Substantial MAP changes in the evolution of novel behaviours have rarely been quantified so we examined MAP differences across strikes, chewing and rakes in a derived raking salmonid, the rainbow trout, *Oncorhynchus mykiss*. Electromyography, including activity onset timing, duration, mean amplitude and integrated area from five feeding muscles revealed significant differences between behaviour-specific MAPs. Specifically, early activity onset in the protractor hyoideus and adductor mandibularis muscles characterised raking, congruent with a recent biomechanical model of the component-mechanisms driving the raking preparatory and power-stroke phases. *Oncorhynchus* raking MAPs were then compared with a phylogenetically derived osteoglossomorph representative, the Australian arowana, *Scleropages jardinii*. In both taxa, early onset of protractor hyoideus and adductor mandibularis activity characterised the raking preparatory phase, indicating a convergently derived MAP, while more subtle inter-lineage divergence in raking MAPs resulted from onset-timing and duration differences in sternohyoideus and hypaxialis activity. Convergent TBA morphologies are thus powered by convergently derived MAPs, a phenomenon not previously demonstrated in feeding mechanisms. Between lineages, differences in TBA morphology and associated differences in the functional coupling of jaw systems appear to be important factors in shaping the diversification of raking behaviours.

Key words: functional decoupling, aquatic feeding, fish, electromyography, sonomicrometry.

INTRODUCTION

The evolution of feeding strategies among aquatic vertebrates is characterised by repeated diversification of prey capture and processing behaviours possibly with accompanying shifts in the muscle-activity patterns governing such strategies. In spite of these repeated trends and the resulting intense focus on muscle-activity patterns of fish feeding, convergently derived muscle-activity patterns (MAPs) have never been documented (Wainwright and Friel, 2001; Wainwright, 2002). Experimental analyses of MAPs in basal vertebrate aquatic feeding have focused on prey-capture behaviours, whereas MAP variability across an extensive range of prey-processing behaviours remains poorly quantified (Grubich and Wainwright, 1997; Grubich, 2001). MAP evolution across prey-capture modes and among feeding behaviours remains enigmatic, despite extensive comparisons of suction-feeding taxa (Grubich, 2001), biting taxa (Friel and Wainwright, 1997; Friel and Wainwright, 1998; Alfaro and Westneat, 1999; Wainwright and Friel, 2000), and biters with ram-suction feeders (Wainwright et al., 1989; Alfaro et al., 2001). Strike MAPs are often highly variable (Wainwright et al., 1989; Alfaro et al., 2001), both at high phylogenetic (among species and above) and at phenotypic levels (among individuals).

Prey processing in a pharyngeal jaw apparatus is by far the best-studied teleost prey-processing mechanism, which has decoupled the oral jaws from mastication tasks and has convergently evolved in several derived (euteleostean) lineages (Sibbing et al., 1986; Wainwright, 1989a; Wainwright, 1998b; Wainwright, 2005; Grubich

and Westneat, 2006). By contrast, functionally coupled feeding mechanisms, although rare, may govern several behaviours without constraining functional versatility, such as prey capture and processing behaviours governed by the oral jaw apparatus in tetraodontids (Wainwright and Turingan, 1993; Van Wassenbergh et al., 2007b). Coupled mechanisms may thus, in contrast with decoupled mechanisms, be useful functional systems for empirical tests of the evolutionary role that MAPs play during functional shifts, ultimately resulting in behavioural–ecological diversification (Alfaro and Herrel, 2001; Wainwright, 2002).

Intra-oral prey-processing mechanisms involving the hyolingual system represent such a coupled system, retaining close musculoskeletal associations with the oral jaw apparatus whilst occurring episodically across the actinopterygian radiation (Lauder, 1980; Lauder and Liem, 1983). The use of clearly distinguishable hyolingual prey-processing behaviours to reduce and immobilise prey make salmonid and osteoglossomorph fishes a particularly interesting case study (Sanford and Lauder, 1989; Sanford, 2001b). A novel raking behaviour, employed by all but a few members in both lineages, is governed by a novel tongue-bite apparatus (TBA), formed by opposing basihyal and oral cavity roof dentition intercalated between the oral and pharyngeal jaws (Sanford, 2001a; Sanford, 2001b; Hilton, 2001; Hilton, 2003). In addition to raking, cyclic intra-oral chewing behaviours are also used by osteoglossomorphs (Sanford and Lauder, 1989; Sanford and Lauder, 1990; Frost and Sanford, 1999) salmonids (Sanford, 2001b) and non-raking neoteleosts (Lauder, 1981).

In earlier studies, raking kinematic data from a phylogenetically diverse range of representatives from both known raking lineages were used to describe two-dimensional biomechanics (Sanford, 2001a; Sanford, 2001b). These mechanisms appear to involve (1) two musculoskeletal pathways driving the raking preparatory phase, and (2) three pathways driving the subsequent raking power stroke. Set in a combined model, these mechanisms predict how a raking preparatory phase 'primes' the TBA *via* basihyal protraction, caused by the protractor hyoideus (PH), or the posterior intermandibularis (PIM) in notopterid osteoglossomorphs (see Greenwood and Lauder, 1981; Sanford and Lauder, 1989). Concurrently, the adductor mandibularis (AM) causes mandible adduction thereby immobilising prey caught inside the mouth (Sanford and Lauder, 1989).

The raking power stroke is initiated with epaxial (EP)-driven cranial elevation, protracting and elevating the TBA upper jaw. Concomitantly, the basihyal (TBA lower jaw) is retracted either directly, by the sternohyoideus (SH) or indirectly, by hypaxial (HP) strain, transmitted *via* a novel cleithrobranchial ligament (CBL) (Sanford, 2001a; Sanford, 2001b; Hilton, 2001). The cleithrobranchial ligament connects the pectoral girdle and basihyal, in parallel with the SH muscle (Fig. 1), and may functionally decouple this muscle during raking (Sanford and Lauder, 1989; Sanford, 2001b), while also possibly influencing more generalised strike and chewing feeding behaviours in these same taxa (Liem, 1970; Lauder, 1980; Sanford and Lauder, 1989; Sanford and Lauder, 1990; Sanford, 2001a; Sanford, 2001b). Interestingly, the SH exhibited a labile feeding MAP compared with four other feeding muscles in the osteoglossomorph *Chitala*, a pattern that extends widely across aquatic feeding vertebrates (Sanford and Lauder, 1989). The combination of a complex TBA morphology and EMG data suggesting a labile MAP emphasises the importance of conducting a direct functional evaluation of the SH–CBL complex.

Video kinematics can provide indirect evidence of isotonic muscle contraction in simple lever systems, such as neurocranial elevation, where only one muscle (epaxial) is functionally capable of causing the movement (Sanford and Lauder, 1989; Carroll, 2004). Deeper, more complex systems require direct recording of muscle activity patterns like the TBA, where anteroventral basihyal protractors (PH/PIM) may antagonise chain-linked basihyal retractor synergists (SH and HP) situated further posteriorly (Fig. 1). The lack of a protractor pectoralis muscles in raking taxa (Greenwood and Lauder, 1981) and the presence of a CBL further increases the system complexity.

Our aim was to provide a first quantitative analysis of feeding behavioural MAPs in representative salmonid and osteoglossomorph taxa where TBA diagnostics and raking involving comparable TBA biomechanics are present, but no quantitative MAP evidence exist, and where size-matched specimens were obtainable, namely the rainbow trout, *Oncorhynchus mykiss* and the Australian arowana, *Scleropages jardinii*. We clarify the specific roles of primary TBA muscles, quantify the MAPs of raking and chewing, alternative forms of intra-oral prey processing, and compare these with strike MAPs.

We were interested in the degree of difference and stereotypy in raking MAPs, relative to other feeding behaviours within and between lineages. Specifically, we examined *O. mykiss* to determine whether (1) salmonid raking MAPs were different from that of strike and chew MAPs? Comparing raking MAPs from *O. mykiss* and *S. jardinii*, we then investigated whether (2) raking MAPs differ between these lineage representatives and (3) if raking may be convergently derived from ancestral feeding patterns? These analyses quantify how variability of MAPs during raking compares

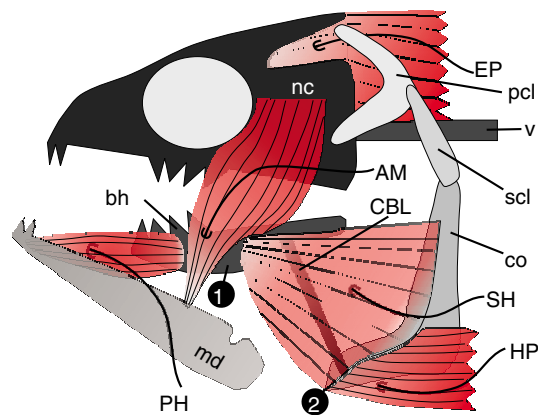


Fig. 1. Diagram of the tongue-bite apparatus (TBA) in a generalized teleost head model, illustrating the five muscles sampled using electromyography in this study. The cleithrobranchial ligament [CBL; situated within the sternohyoideus (SH) muscle] and the positions where two sonomicrometric crystals (1, 2) were sutured to monitor relative CBL distance during feeding in *O. mykiss* are shown. Other muscle labelling: AM, adductor mandibularis; EP, epaxialis; HP, hypaxialis; PH, protractor hyoideus. Bone labelling: bh, basihyal; co, coracoid; md, mandible; nc, neurocranium; pcl, post-cleithrum; scl, supracleithrum; v, vertebral column.

to changes at other organisational levels, including morphology and kinematics. A notion exists in the literature that raking kinematics are comparable to a closed-mouth strike (Sanford and Lauder, 1990; Sanford, 2001b). Following this notion, we hypothesise that temporal muscle-activity variables that distinguish raking from more general feeding behaviours such as the strike are convergently derived in both of the known raking lineages.

MATERIALS AND METHODS

Specimen and husbandry

Size-matched rainbow trout [*Oncorhynchus mykiss* Walbaum; $N=5$, head lengths (HL)=50–59 mm, mean \pm s.e.m., 55 ± 0.894] were obtained from the Cold Spring Harbour fish hatchery, Long Island New York. Australian arowanas [*Scleropages jardinii* (Saville-Kent); $N=5$, HL=52–61 mm; mean 55 ± 0.853] of a similar size (t -test; $P=0.948$) were purchased from local aquarium stores. All specimens were housed individually in the Hofstra University animal care facility, in accordance with applicable ethics approvals and animal-care protocols. Trout were kept at $15\pm 2^\circ\text{C}$ and arowana at $27\pm 2^\circ\text{C}$, both in a 12 h:12 h light:dark photoperiod, as per previous studies (Ojanguren and Brana, 2000; Sanford, 1990; Sanford, 2001b). During acclimation, individuals were fed a varied diet of crickets (*Gryllus* sp.), goldfish (*Carassius* sp.), earthworms (*Lumbricus* sp.) and minnows (*Pimephales* sp.) to avoid habituation. Experiments were commenced when individuals were well acclimated and fed vigorously under floodlight illumination with no signs of hesitation in front of the provisioner. In order to standardise the motivation level among individuals and experiments we did not feed specimens for 2 days prior to each experiment.

Electromyography recording

Electromyography (EMG) recordings were taken from five muscles that are commonly involved in vertebrate aquatic feeding (Wainwright et al., 1989; Grubich, 2001) and have been argued to be important during raking (Sanford and Lauder, 1989; Sanford, 2001a; Sanford, 2001b), namely the sternohyoideus (SH), protractor hyoideus (PH), adductor mandibularis (AM), epaxialis (EP), and

hypaxialis (HP) muscles. We used a modified protocol from Wainwright et al. (Wainwright et al., 1989) and Alfaro and Westneat (Alfaro and Westneat, 1999). Hooked fine-wire electrodes were prepared by threading 1.25 m lengths of bi-filar wire (0.05 mm diameter polyethylene-coated stainless steel; California Fine Wire, Grover Beach, CA, USA) through 25 5/8 hypodermic needles. Electrodes were implanted at a 45° angle to the surface of the left side muscles of anaesthetised animals (40 p.p.m. alcoholic Eugenol, Rush & Hebble, Edinburgh, IN, USA) (Munday and Wilson, 1997). During implanting, the hooks were anchored percutaneously into the muscle bellies, parallel to the muscle fibre orientation. Electrode wires were anchored to a mid-dorsal suture on the specimen, joined with glue while the electrode connector ends were crimped into din-25 adaptor pins, and floats were taped to the electrode wires to prevent tangling of specimens. Surgery lasted ~20 min, and specimens recovered totally ~45 min after surgery onset.

Difficulties with obtaining size-matched specimens meant that several experiments had to be conducted on each specimen (see below). Owing to the large specimen size, muscles of interest were large, easily identifiable and clearly delineated. Thus, instead of verifying electrode placement in dissections following experiments, we conducted repeated-practice implants on freshly thawed specimens from each species, and used dissections to verify electrode placements in these. During experiments, prey, consisting of live goldfish, approximating lateromedial gape width of the specimen sampled (35–40 mm total length *TL*), were released with the predator, which typically caught the prey instantaneously using a rapid ram-suction feeding strike. Electrical signals produced by muscle activity during prey capture and processing were sampled at 4 kHz, amplified 1000 times (A-M systems, differential AC amplifier, model 1700, Everett, WA, USA), and conditioned with band-pass at 1000–100 Hz with a 60 Hz (notch) filter engaged. EMG signals, and a manual trigger code (+5 V) used to label the

behaviours during recording, were digitized using a PowerLab 16/30 system linked to a PC running Chart v.5.4 for Windows (PowerLab, Colorado Springs, CO, USA). After each feeding trial, signals were comprehensively logged for, e.g. behaviour type, prey orientation and predator motivation, using the comments tool in Chart. In order to focus on the level of inter-lineage stereotypy in behaviourally related MAPs we used replicate events ($N=5$) from more individuals ($N=5$) than is commonly used in MAP studies, thus allowing more accurate quantification of intra-specific motor-pattern variability (e.g. Wainwright et al., 1989). Although we observed the predator feeding on several prey items aggressively before any effects of satiation were evident, we only selected video sequences from the first three feedings of each experiment for analysis.

EMG data extraction and derived variables

We selected EMG signals for analysis based on evaluations of predator voracity and other relevant information retrieved during data collections. From rectified EMG signals of the five muscles sampled, we measured a total of 20 different MAP variables, which can be divided into five groups: (1) muscle activity duration (ms); (2) relative MAP onset (ms), relative to EP muscle onset time (reference muscle); (3) mean amplitude (signal intensity; in mV), corrected with the maximum recorded activity (spike) from that muscle for that implant across behaviours; and (4), integrated area (signal energy), i.e. 'area under the curve', but above the signal baseline, in mV*s, corrected with the same maximum amplitude spike; and finally, (5) total duration of behaviour i.e. the duration from onset timing of first to offset timing of last muscle activity during one behavioural bout was also quantified (Table 1) but not included in further analyses.

Recruitment variables were analysed with and without spikes and using binning of 10 ms time intervals for a subset of the data, all of which resulted in no significant differences (ANOVA; $P=0.12$).

Table 1. Summary of 20 electromyographic variables across three behaviours in *O. mykiss* and two behaviours in *S. jardinii*

Variable	Rake		Strike		Chew
	<i>O. mykiss</i>	<i>S. jardinii</i>	<i>O. mykiss</i>	<i>S. jardinii</i>	<i>O. mykiss</i>
Relative onset timing relative to EP onset (ms)					
SH relative onset	25.73±3.61	-32.31±3.43	-23.79±6.22	0.26±1.30	-5.76±2.88
PH relative onset	-91.82±5.88	-92.70±7.61	92.89±11.34	9.31±2.65	61.46±5.49
AM relative onset	-61.19±3.50	-65.36±6.99	51.79±4.84	14.86±4.10	32.24±2.33
HP relative onset	25.38±2.42	-16.62±3.81	-5.82±3.22	-0.52±0.77	-2.00±0.60
Activity duration (ms)					
SH duration	41.08±3.84	79.83±5.20	92.39±10.26	38.28±4.75	34.46±3.72
PH duration	88.32±5.37	129.64±7.82	136.36±21.89	51.24±5.18	100.25±9.05
AM duration	81.67±3.86	98.27±6.98	182.36±25.02	90.56±11.07	110.91±10.53
EP duration	49.81±1.59	45.36±2.02	54.04±4.87	37.75±4.58	27.53±2.16
HP duration	28.32±2.81	61.64±4.10	67.41±8.06	35.83±4.26	28.55±2.29
Corrected mean amplitude (mV ratio)					
SH mean amplitude	0.06±0.01	0.04±0.01	0.12±0.02	0.13±0.03	0.11±0.01
PH mean amplitude	0.12±0.02	0.11±0.01	0.06±0.01	0.09±0.02	0.10±0.01
AM mean amplitude	0.09±0.01	0.09±0.01	0.08±0.01	0.11±0.01	0.07±0.01
EP mean amplitude	0.07±0.01	0.11±0.01	0.10±0.01	0.12±0.02	0.10±0.01
HP mean amplitude	0.10±0.01	0.02±0.00	0.09±0.01	0.15±0.01	0.08±0.01
Integrated area (mV*s)					
SH integrated area	0.48±0.07	1.61±0.48	3.21±0.53	1.23±0.19	1.32±0.18
PH integrated area	5.06±0.73	8.52±0.88	2.15±0.48	2.85±0.57	4.23±0.57
AM integrated area	5.12±0.76	3.92±0.55	8.97±2.07	8.61±2.07	5.27±0.75
EP integrated area	1.37±0.18	3.06±0.22	1.78±0.31	2.45±0.23	1.10±0.15
HP integrated area	0.62±0.04	0.89±0.11	1.01±0.12	3.99±0.70	0.68±0.09
Total duration of behaviour (ms)	159.99±32.00	150.51±30.10	274.33±54.87	109.97±21.99	176.40±35.28

For explanation of variables, see text. Total duration of rake cycle was not used for parametric analyses. Values are means ± s.e.m.

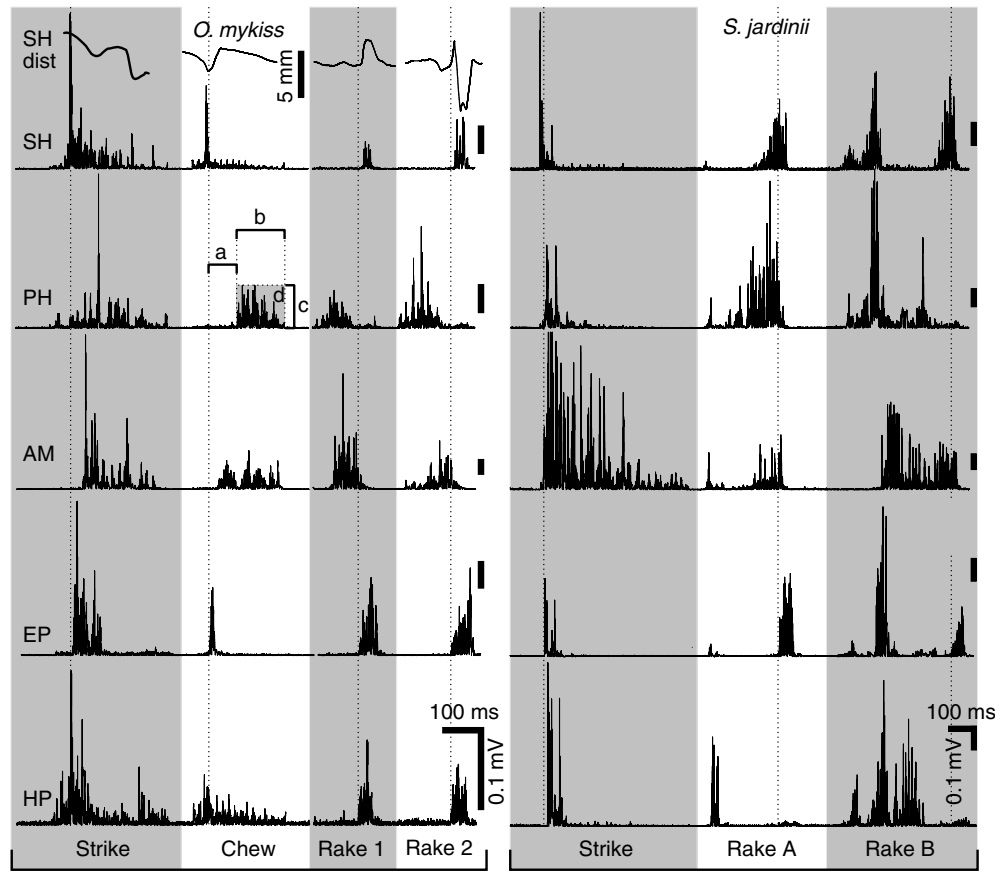


Fig. 2. Rectified electromyograms representing typical raw data from feeding behaviours in *O. mykiss* (left) and *S. jardinii* (right). Data for five sampled muscles are shown: SH, sternohyoideus; PH, protractor hyoideus; AM, adductor mandibularis; EP, epaxialis; HP, hypaxialis. Measured variables are indicated with brackets: a, activity onset time, relative to EP activity onset (vertical dotted lines); b, activity duration; c, activity mean amplitude [in analyses corrected with highest muscle-specific amplitude (spike) during an experiment]; d, integrated area, an intensity measurement of the area defined by the rectified curve and the baseline of the muscle activity signal (grey shading). In *O. mykiss*, SH dist. is sonomicrometry data on strain, measured with two piezoelectric electrodes sutured to the ventral coracoid and urohyal keels, at the sternohyoideus origin and insertion. Note that in some rakes (rake 1) SH activity does not equal contraction and SH stretching results from HP or PH activity. In other rakes, exhibiting greater SH activity (rake 2), the initial stretching is compensated for by much higher levels of SH activity. In *S. jardinii*, isolated chewing behaviour is uncommon and not illustrated, whereas raking is preceded by muscle activity driving a ubiquitous prey repositioning behaviour with EMG profiles closely resembling chewing EMG profiles (see *O. mykiss*). We only analysed raking EMG data that were clearly distinguished from this early behaviour (by at least 50 ms pause in activity for all muscles; rake A). Less discreet behaviour complexes (rake B) were omitted from analysis.

Thus our original data was used without removal of spikes or binning. Parametric analyses were initially performed on corrected and non-corrected variables, and integrated area was the only variable group for which the resulting PC-factor scores and component loadings did not differ. To retain potentially important biological information in the dataset, final parametric analyses used uncorrected integrated area values.

Sonomicrometry recording

The contribution by sternohyoideus muscle contraction to feeding kinematics is poorly quantifiable using conventional (high-speed video) methods, given the medial placement of this muscle and the hyoid apparatus relative to the mandible, opercular series and suspensorium. Also, inferences about muscle strain cannot reliably be made from electromyography (Carroll, 2004). Therefore, in two *O. mykiss* we sutured two 2 mm piezoelectric crystals (Sonometrics Corp., London, ON, Canada) to the ventral coracoid and urohyal keels (Fig. 1), at the sternohyoideus origin and insertion ends, respectively. The keels provide an accurate measure of SH length while minimising invasive surgery. As a proxy of SH length, this

configuration of crystal placement would also provide evidence of dynamic tension on the CBL exerted during activity in the PH (anterior) and HP (posterior). During EMG electrode implantation, the mid-ventral region surrounding the sternohyoideus muscle was palpated to locate the bony elements immediately under the integument, to which the crystals were sutured through integument and bone. The sturdiness of crystal attachment was verified by vigorous expansive and compressive head manipulations on the anaesthetised fish. Sonomicrometry data was inspected in SonoView (Sonometrics Corp., London, ON, Canada) and the analogue sonometric signals were simultaneously recorded on the EMG PowerLab system, where they were calibrated and converted to mm (Fig. 2).

Statistical design

We computed means and standard errors from all EMG variables across species-specific behaviours (trout strike, chew and rake; arowana strike and rake; Table 1), presented in box plots of species-specific behaviours (Fig. 3), but parametric analyses used derived, non-averaged data. This study aimed at answering three major

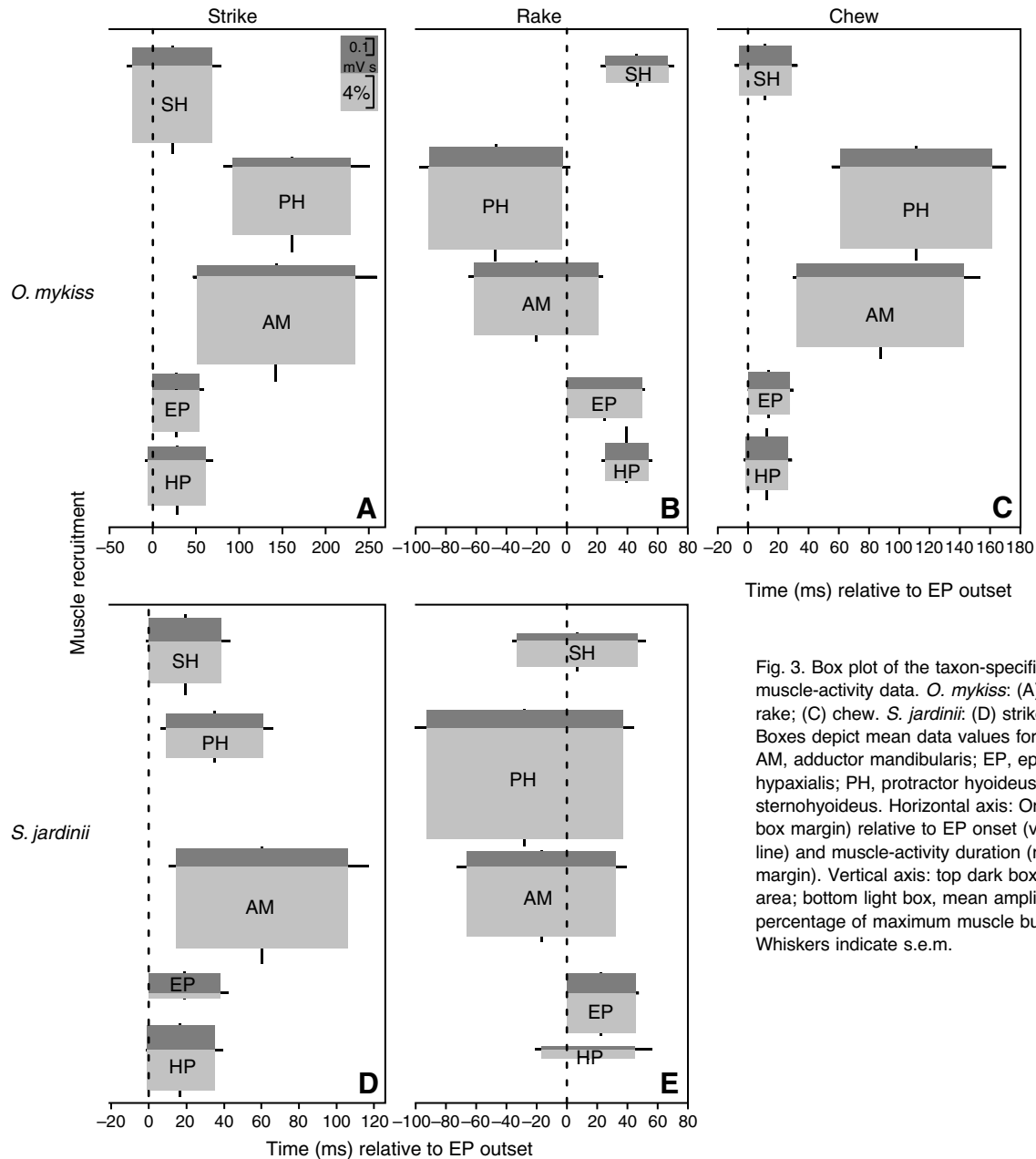


Fig. 3. Box plot of the taxon-specific behavioural muscle-activity data. *O. mykiss*: (A) strike; (B) rake; (C) chew. *S. jardinii*: (D) strike, (E) rake. Boxes depict mean data values for one muscle: AM, adductor mandibularis; EP, epaxialis; HP, hypaxialis; PH, protractor hyoideus; SH, sternohyoideus. Horizontal axis: Onset-time (left box margin) relative to EP onset (vertical dotted line) and muscle-activity duration (right box margin). Vertical axis: top dark box, integrated area; bottom light box, mean amplitude as a percentage of maximum muscle burst per implant. Whiskers indicate s.e.m.

questions regarding raking behaviours and the underlying muscle-activity patterns. We segregated our statistical analyses accordingly, using a parametric statistical design incorporating a principal component analyses (PCA) on the covariance matrices (eigenvalues >1), with a MANOVA on PC factor scores for the entire dataset. Subsequently, ANOVAs on factor scores for each axis and Bonferroni-corrected *post-hoc* tests were used to determine which behaviours, if any, differed.

Scatter plots of the informative PC axes resulting from the 19 derived MAP variables (total MAP duration not analysed) illustrated the distribution of species-specific behaviours relative to MAP similarities and differences. In biplots of informative PC axes, the most influential component loadings (for covariance matrices, values over 15), were scaled to PC axis length and superimposed in order to identify the most important variables in segregating species-specific behaviours across available multivariate MAP space.

To test the overall hypothesis that the MAPs governing the three behaviours, strike, chew and rake, are different in *O. mykiss* we ran a PCA to identify informative axes of variation (eigenvalues >1), followed by a MANOVA. To ascertain which behaviours differed significantly, we used ANOVAs on PC factor scores for each principal component axis followed by *post-hoc* tests using Bonferroni-corrected comparisons with behaviour as the fixed main effect and the interaction term (behaviour \times individual) as the denominator in calculating the mean-square error (Zar, 1999). This design identifies significant PC axes and behavioural differences along them, whilst accounting for the effects caused by individual variability.

To test whether raking MAPs differ between lineages, we analysed the EMG data from *O. mykiss* and *S. jardinii* using a PCA analysis and a nested MANOVA design with species as the fixed main effect [following Zar (Zar, 1999)].

In order to determine whether raking MAPs overall are convergently derived from the remaining feeding behaviours utilised

Table 2. Summary of PC loadings from a principal component analysis on 19 muscle-activity patterns variables describing strike, chew and rake feeding behaviours in *O. mykiss*

Variance explained	Principal component loadings			
	PC1 55.5%	PC2 27.7%	PC3 7.4%	PC4 3.9%
MAP variables				
Adductor mandibularis activity duration	78.47	37.12	-7.16	-16.73
Protractor hyoideus onset timing	70.08	-55.49	8.18	-7.90
Protractor hyoideus activity duration	48.45	48.50	12.46	17.40
Adductor mandibularis onset timing	38.79	-27.60	10.01	17.75
Hypaxialis activity duration	18.09	2.07	-9.20	1.68
Sternohyoideus activity duration	15.98	-8.38	-36.41	7.73
Sternohyoideus onset timing	-15.54	11.04	14.70	-8.51
Hypaxialis onset timing	-9.45	9.39	-0.75	-3.55
Adductor mandibularis integrated area	4.43	4.14	0.30	-0.03
Sternohyoideus integrated area	3.51	0.66	-2.48	1.66
Epaxialis activity duration	2.82	5.30	-9.95	2.63
Protractor hyoideus integrated area	2.81	5.38	0.81	0.26
Hypaxialis integrated area	1.91	0.61	-0.33	0.04
Epaxialis integrated area	1.15	0.94	-0.42	0.81
Sternohyoideus mean amplitude	0.03	0.02	0.01	0.01
Epaxialis mean amplitude	0.02	0.01	0.01	0.01
Protractor hyoideus mean amplitude	-0.02	0.01	0.00	-0.02
Hypaxialis mean amplitude	-0.01	0.00	0.01	-0.01
Adductor mandibularis mean amplitude	-0.01	0.01	0.01	0.01
F-statistics ($F_{2,72}$)	58.16, $P<0.001^*$	16.53, $P<0.001^*$	15.19, $P<0.001^*$	2.73, $P=0.07$
Rake ≠ chew	$P<0.05^*$	$P=0.08$	$P=0.13$	
Rake ≠ strike	$P<0.001^*$	$P=0.15$	$P=1.00$	
Chew ≠ strike	$P=0.13$	$P=1.00$	$P=0.13$	

Summary ANOVAS and Bonferroni-corrected *post-hoc* test *P* values along PC axes are also given.

*Significant after Bonferroni correction

MAP, muscle-activity pattern; bold type signifies, high PC loadings (see text) and significant *P*-values.

by the species studied, we ran a PCA on the covariance matrix of the complete dataset, excluding chewing data from *S. jardinii*, which did not reach the required sample size because of infrequent use of this behaviour. Evolutionary differences in MAPs were distinguished from significant individual and species effects, using a mixed-model MANOVA with species as a fixed, and individual within species as a random effect.

RESULTS

Comparison of feeding behaviour MAPs in *Oncorhynchus mykiss*

The duration of rakes (160 ± 32 ms; mean \pm s.e.m.) and chews (176 ± 35 ms) in *O. mykiss* were not significantly different, and both lasted significantly shorter than the average strike (ANOVA; $P<0.001$) (Table 1). Statistically different MAPs characterise the three feeding behaviours (MANOVA: Wilk's $\lambda=0.039$, $F_{8,138}=70.221$, $P<0.001$) and a PCA on the 19 derived EMG variables from all *O. mykiss* feeding behaviours is summarised in Table 2. Timing and duration variables are overriding in distinguishing raking from other feeding behaviours, compared with amplitude and integrated area variables. Specifically, early protractor hyoideus (PH) and adductor mandibularis (AM) onset-timing characterises raking MAPs (Fig. 3A–C, Table 1).

The PCA recovered four informative PC axes and ANOVAs on the PC factor scores, with Bonferroni-corrected *post-hoc* tests run separately on each axis, showed that the raking MAP differs from strike and chewing along PC1 only, whereas the two latter behaviours were not statistically different (Table 2). A scatter plot of PC1 and 2 (Fig. 4A) illustrates that the *O. mykiss* raking MAP occupies a distinct region of multivariate MAP space, primarily driven by an

early onset in AM and PH activity during raking, while differences in AM and PH activity durations separate strike and chew MAPs.

Raking is governed by a much more stereotypical MAP than other feeding behaviours, as illustrated by the tight cluster of raking PC factor scores (Fig. 4A), and by a very restricted variation in MAP among individuals along PC1 relative to chewing and in particular strike MAPs (Fig. 4B). The strike MAP factor scores displaced towards high positive values along PC1 belong to one individual of a statistically similar size to the four other individuals. Running analysis without strikes for that individual gave very similar percentages of variance explanation along PC axes. Duration of SH activity was the only MAP variable driving significant variation among feeding behaviours along PC3 (Table 2).

Sternohyoideus–cleithrobranchial ligament complex

Although SH mean amplitude did not influence the PCA for *O. mykiss*, differences between rakes and chews were evident (ANOVA, $P<0.05$), in correspondence with qualitative SH amplitude differences (Fig. 2) between the different behaviours (Table 2). Measurements of SH length changes obtained *via* sonomicrometry indicated that during rakes with low SH amplitude (Fig. 2, rake 1); the SH–CBL complex was stretched by approx. 2% of SH resting length – reliably indicating the absence of SH shortening. Meanwhile, in rakes with higher SH amplitude (Fig. 2, rake 2), initial SH stretching was subsequently recovered *via* SH contraction.

Comparison of raking MAPs in *O. mykiss* and *S. jardinii*

In contrast to *O. mykiss*, the mean rake duration in *S. jardinii* (151 ± 30 ms; mean \pm s.e.m.) was significantly longer than the mean

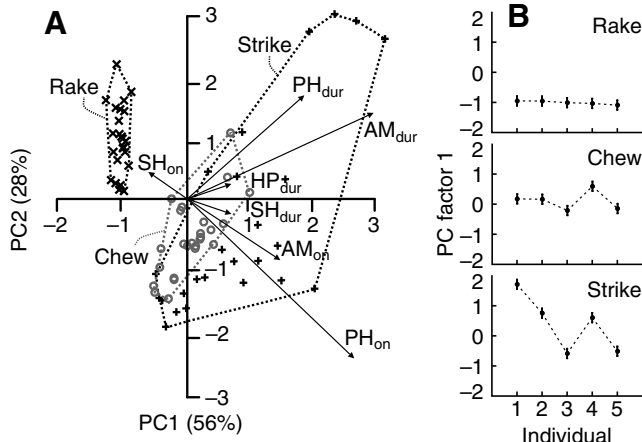


Fig. 4. (A) Scatter plot of PC1 and PC2 from a principal component analysis on trout data, showing the relationship between prey capture (striking), chewing and raking behaviour MAPs in *O. mykiss*. (B) PC1 factor scores for each individual ($N=5$) across all three feeding behaviours, illustrating the stereotypy of raking relative to strike and chew. For muscle abbreviations, see List of abbreviations; on, onset; dur, duration.

strike duration (110 ± 22 ms; t -test, $P < 0.01$; Table 1). Chewing is a relatively uncommon behaviour in *S. jardinii* and is therefore not treated here. Raking MAPs in *O. mykiss* and *S. jardinii* were statistically different (MANOVA: Wilk's $\lambda = 0.17$, $F_{4,5} = 55.119$, $P < 0.001$), and a principal component analysis recovered four PC axes, summarised in Table 3. A subsequent ANOVA on the PC factor scores (Table 3) determined that raking MAPs between the two species differ along PC1–3, and a scatter plot of axes 1 and 2 (Fig. 5) show raking behaviour separation across multivariate MAP space.

Raking in both *O. mykiss* and *S. jardinii* is characterised by early onset in PH and AM activity, while an extended duration of activity in these muscles during *S. jardinii* raking is the most significant discriminator of inter-specific raking MAPs. Inter-specific differences in raking behaviours are also driven by earlier onset and longer lasting activity duration in *S. jardinii*, of the ventral muscles driving pectoral girdle retraction (HP) and direct basihyal retraction (SH) during the raking power stroke (Table 1; Fig. 3). During *S. jardinii* raking, activity in these muscles is also characterised by relatively low, although not significantly different mean amplitude and integrated area means compared to *O. mykiss* (Fig. 3).

Comparison of MAPs governing all species-specific feeding behaviours

Rakes are shorter than strikes in *O. mykiss* but longer than strikes in *S. jardinii* (t -test, $P < 0.01$; Table 1), whereas mean rake duration in *O. mykiss* and *S. jardinii* was very similar (t -test, $P = 0.403$; Table 1). Mean duration of SH and HP muscle activity in *S. jardinii* is longer during rakes than during strikes, whereas the opposite is the case in *O. mykiss* (Table 1, Fig. 3). Given these inter-specific MAP-duration differences, the divergent inter-specific relationships in SH and HP muscle duration between rakes and strikes were confirmed by calculating total behaviour-duration-corrected muscle activity means, which did not differ from non-corrected means (Table 1).

All rakes investigated had a different onset profile than the more generalised feeding behaviours (strike and chew; Fig. 3). Raking was primarily driven by early mean onset times in the PH and AM muscles relative to the onset of EP activity. In more generalised behaviours both PH and AM muscles lag behind the EP. A principal component analysis on the covariance matrix of 19 transformed data variables for all inter-specific feeding behaviours analysed explained 91.5% of the total variation in the dataset. Three principal components with Eigenvalues over 2.0 were recovered, explaining

Table 3. Summary of a principal component analysis on 19 muscle-activity pattern variables comparing raking feeding behaviours in *O. mykiss* and *S. jardinii*

Variance explained	Principal component loadings			
	PC1	PC2	PC3	PC4
Variance explained	51.4%	18.5%	18%	6.1%
MAP variables				
Protractor hyoideus activity duration	-34.72	15.18	6.00	3.12
Sternohyoideus onset timing	27.22	6.72	17.26	5.90
Sternohyoideus activity duration	-23.14	2.69	-13.06	-11.48
Protractor hyoideus onset timing	21.35	-17.30	-17.81	0.96
Hypaxialis onset timing	19.25	10.69	7.32	-11.41
Hypaxialis activity duration	-18.98	-5.84	-3.62	11.44
Adductor mandibularis activity duration	-14.33	-18.62	15.49	-3.24
Adductor mandibularis onset timing	10.56	18.02	-16.32	4.87
Protractor hyoideus integrated area	-1.81	1.08	-0.55	-0.44
Sternohyoideus integrated area	-0.86	-0.77	0.51	0.34
Epaxialis integrated area	-0.68	0.05	-0.45	0.46
Adductor mandibularis integrated area	-0.66	-1.68	1.19	0.36
Epaxialis activity duration	0.46	5.24	1.11	0.52
Hypaxialis integrated area	0.45	0.05	0.62	-0.02
Hypaxialis relative mean amplitude	0.04	0.01	0.02	-0.01
Protractor hyoideus mean amplitude	0.02	-0.00	-0.01	-0.01
Epaxialis mean amplitude	-0.02	-0.01	-0.01	0.01
Adductor mandibularis mean amplitude	0.01	-0.00	-0.00	0.01
Sternohyoideus mean amplitude	0.00	-0.01	0.02	0.01
F-statistics ($F_{1,40}$)	71.0, $P < 0.001$	8.20, $P < 0.01$	22.54, $P < 0.001$	1.10, $P = 0.3$

Nested MANOVA results for each PC axis, excluding the effect of individual variability, are also given.

MAP, muscle-activity pattern; bold type signifies high PC loadings (see text) and significant P -values.

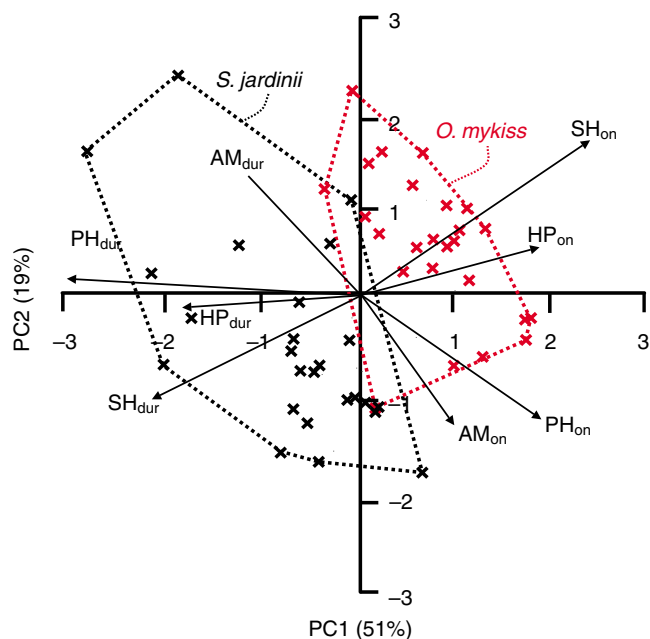


Fig. 5. Scatter plot of PC1 and PC2 from a principal component analysis on raking data, investigating the behavioural differences between *O. mykiss* and *S. jardinii*. For muscle abbreviations, see List of abbreviations; on, onset; dur, duration.

53.1%, 21.3% and 10.9% of the variation, respectively. Raking behavioural MAPs occupy a completely distinct region of multivariate space from strike and chewing behaviours, the latter polygons of which largely overlap (Fig. 6). The principal variables driving this noteworthy displacement of raking MAPs in both taxa are early onset timings of AM and PH musculature, which occurs in both taxa (Fig. 3).

Furthermore, the variables separating *O. mykiss* and *S. jardinii* raking centre on differences in activity duration in the AM and PH musculature, both lasting shorter during *O. mykiss* raking, while remaining active during the raking power-stroke MAP of *S. jardinii*. The areas of species-specific behaviour polygons indicate the relative degree of stereotypy in species-specific behaviours (Fig. 6): raking is clearly governed by a restricted degree of MAP variability in both taxa, while, for example, MAPs of trout strikes are particularly variable. However, whereas raking is particularly stereotypical in *O. mykiss*, early preparatory phase variation often occurs in *S. jardinii*, as an initial burst of activity in all muscles, prior to PH activity onset (rake B, Fig. 2).

DISCUSSION

Variation in MAPs among strike, chewing and raking behaviours in *O. mykiss*

Clear distinctions were found between the muscle activity pattern (MAP) of raking, and the more similar, and generalised, strike and chewing behaviours. The most divergent MAP traits were early activity onset during raking in the protractor hyoideus (PH) and adductor mandibularis (AM) muscles. This corresponds well with early onset of jaw adduction and basihyal protraction characteristic of the raking preparatory phase (Sanford and Lauder, 1989; Frost and Sanford, 1999; Sanford, 2001a; Sanford, 2001b). Although Sanford and Lauder (Sanford and Lauder, 1989) distinguished raking from strike and chewing in the basal osteoglossomorph *Chitala*, MAPs of

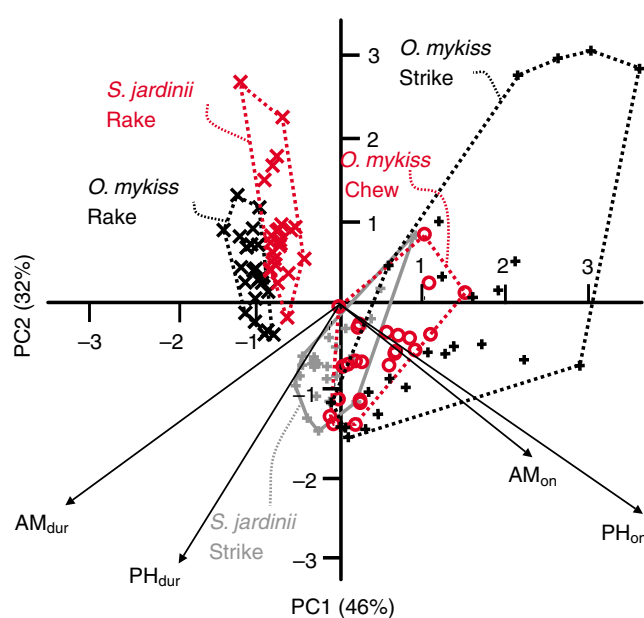


Fig. 6. Scatter plot of PC1 and PC2 from a principal component analysis on the covariance matrix of the full dataset showing the distribution and occupation of MAP two dimensional space by the five species-specific behaviours analysed. For muscle abbreviations, see List of abbreviations; on, onset; dur, duration.

the latter two behaviours were also significantly different. However, this finding could be explained by differences in EMG protocol used by Sanford and Lauder (Sanford and Lauder, 1989). Differences in EMG protocol prevent direct comparison of our results with *Chitala*, as Sanford and Lauder (Sanford and Lauder, 1989) used maximum amplitudes, while omitting amplitude correction for implant. Nevertheless, it is now clear that raking MAPs in representative taxa from both known raking lineages thus far studied differ from strike and chewing MAPs.

From a functional perspective, the differences between behaviour-specific MAPs closely match the biomechanical prerequisites of the different behaviours. Raking entails preparatory, power-stroke and recovery phases (Sanford, 2001a; Sanford, 2001b), much like the basal-most vertebrate aquatic prey-capture mechanism, the suction-feeding strike that also involves such consecutive phases (Liem, 1978; Lauder, 1985; Shaffer and Lauder, 1985; Lauder and Reilly, 1994; Reilly, 1995; Motta et al., 1997). During the raking preparatory phase, PH-driven basihyal protraction 'primes' the TBA, while the prey is retained and compressed in the oral cavity by AM-driven oral jaw occlusion, preventing its escape. Oral jaw occlusion may also optimise the trajectory of subsequent basihyal retraction during the power stroke (Sanford and Lauder, 1989). Conversely, early AM and PH activity onset during strike or chewing behaviours would prevent prey capture and mastication, whereas both may be involved in slow oral jaw occlusion post-strike, provided the line of action of the PH has swung dorsal to the lower jaw joint (Lauder, 1981). Certainly, this occurs in *S. jardinii* during raking, and maintained PH activity may thus be contributing to the firm mandible occlusion seen throughout the raking power stroke in this, and other osteoglossomorph taxa examined to date (Sanford and Lauder, 1989; Sanford, 2001a). Overall, raking contrasts with strike and chewing behaviours, both in terms of biomechanical and neuromotor physiological characteristics, whilst minimising the proximal

constraints on prey acquisition and offering an alternate avenue of prey processing.

Clearly, AM and PH activity variables, whilst primarily governing the raking preparatory phase, play overriding roles both in distinguishing raking MAPs from other feeding behaviours, and also distinguishes inter-lineage raking MAPs in this study. Future analyses of raking MAPs from a broader species range should involve parametric comparisons both with and without PH and AM variables, to establish if more subtle MAP differences exist in the feeding muscles more directly involved in the raking power stroke.

Raking MAP comparison

Raking MAPs remained subtly distinct between *O. mykiss* and *S. jardinii*, primarily because of shorter durations of AM and PH activity in *O. mykiss*. The significantly longer PH activity duration in *S. jardinii* provides at least a partial explanation of the reduced posterior pectoral girdle excursion compared to *O. mykiss*. Maintained PH contraction from the preparatory phase into the power stroke (Fig. 3), i.e. overlapping with basihyal retractor musculature activity, may result in tension in this protraction component of the muscular sling suspending the basihyal, thus influencing force transmission from the power-stroke musculature to the basihyal. Alternatively, oral jaw occlusion can result in dorsally directed compressive forces of the basihyal. The prominent anterodorsal oral-cavity incline in *S. jardinii* means that prolonged PH tension, in synchrony with SH and HP contraction (Fig. 3), can result in a dorsally directed crushing action of the basihyal toothplate against the dorsal toothplates in *S. jardinii*. Interestingly, toothplate morphology in *S. jardinii*, more closely resembles crushing pharyngeal plates than the caniniform basihyal fangs in *O. mykiss*, providing morphological evidence that crushing may be the primary osteoglossid TBA function. In *O. mykiss*, evidence of a posteriorly directed shearing action of the basihyal fangs during raking is provided by the fact that SH and HP activity commences well after AM and PH activity, and lasts for a significantly shorter time during raking than during strikes.

Raking kinematics in *S. jardinii*, and likely in other osteoglossids, involves a complex preparatory phase compared to salmonids, with a bipartite pattern of activity associated with intra-oral prey manipulation prior to raking (rake B in Fig. 2). In 254 rake EMGs, from five *S. jardinii*, such bipartite muscle activity was not temporally distinguishable from the main rake EMG in 104 cases (41%), primarily occurring in three individuals during particularly aggressive trains of prey-processing behaviour. In general, a synchronous onset of the SH and HP early in the raking MAP of *S. jardinii* supports the observation that the cranium is noticeably depressed in osteoglossids during the preparatory phase (Sanford and Lauder, 1990). Also, the late onset of EP relative to SH and HP contrasts with the rake MAP in *O. mykiss*, suggesting that in *S. jardinii* basihyal compression–retraction is occurring before the cranium is elevated. Overall, this MAP complexity corresponds well with the kinematic patterns observed in *S. jardinii* (N.K. and C.P.J.S., unpublished data) and its close osteoglossid sister taxa during raking (Sanford and Lauder, 1990). In osteoglossids, neurocranial and pectoral girdle excursions were restricted, whilst oral jaw occlusion and hyoid adduction was more pronounced compared to existing salmonid raking data (Sanford, 2001b). In osteoglossids, this unique combination of raking kinematics probably results in a composite compression and grinding action of the basihyal against the millstone-shaped oral roof. This

composite action clearly diverges drastically from the unidirectional prey shredding commonly hypothesised to result from basihyal kinesis during raking in previous studies. Thus, sonomicrometry will be particularly useful when investigating the functional differences in deep basihyal kinesis across morphologically divergent raking taxa.

The anatomical basis for variation in raking MAPs

Inter-specific raking MAP differences include SH and HP variables, prompting the question of whether functional decoupling is linked to different architectures of a novel cleithrobranchial ligament (CBL) found in the midline, embedded in the SH muscle. Specifically, the CBL origin-insertion trajectory differs between species, with a linear CBL architecture linking the pectoral girdle to the third hypobranchial in *S. jardinii* (N.K. and C.P.J.S., personal observation). This CBL may be an efficient pathway for transmission of HP strain to basihyal retraction, while permitting decoupling of the SH to modulate basihyal power-stroke kinesis. Considering the labile MAP of SH muscles in basal aquatic vertebrates (Carroll, 2004; Van Wassenbergh et al., 2007a), convergent CBL formations may in fact represent evolutionary enhancements to an existing musculoskeletal pathway.

The peculiar curved CBL in *O. mykiss*, inserting partially onto the third hypobranchial tip and predominately onto the dorsocaudal margin of the dorsal hypohyal (N.K. and C.P.J.S., personal observation), may perform differently to the CBL of *S. jardinii* in transmission of HP strain. This interpretation is corroborated by our synchronous sonomicrometry and EMG recordings: manipulation of cleared and stained specimens revealed that approx. 2% SH stretching, the commonly observed SH stretch magnitude in our sonomicrometry data for *O. mykiss* (Fig. 2), resulted in a straight CBL, making it functionally capable of direct HP strain transmission to retract the basihyal. Among such diverse suction-feeding taxa as centrarchids (Carroll, 2004) and clariids (van Wassenbergh et al., 2005) SH stretching is known to occur during strikes, except in taxa with a massive SH (van Wassenbergh et al., 2007a). SH activity variability extends across all feeding behaviours in a broad range of basal aquatic-feeding vertebrates (Wainwright et al., 1989), basal teleosts (Lauder, 1980); scarines (Alfaro et al., 2001), caracoids (Lauder, 1981), centrarchids (Carroll, 2004; Carroll et al., 2004; Carroll and Wainwright, 2006), clariids (Van Wassenbergh et al., 2005; Wassenbergh et al., 2006; Wassenbergh et al., 2007a; Wassenbergh et al., 2007c) and balistids (Wainwright and Turingan, 1993). Accordingly, a curved CBL may represent a trade-off in TBA coupler-linkage architecture to facilitate more efficient suction feeding (by allowing the SH to stretch) in salmonids compared with *S. jardinii*.

Understanding the nature and diversity of this potential decoupling pathway, and the relative contribution from three complementary biomechanical mechanisms to TBA function in salmonids and osteoglossomorphs will be key in future studies. These should focus on quantifying the relative contribution from morphological, mechanical and functional diversity in the convergent evolution of novel raking feeding behaviours. Synchronised use of EMG, sonomicrometry and high-speed video is a powerful tool, which will help to quantify the effect of having a CBL decoupling the SH during raking. Whatever the role of the CBL, the observation that such a ligament is present only in TBA-bearing taxa (Sanford and Lauder, 1989) suggests that its role is primarily driving the control of prey-processing behaviours associated with the TBA rather than oral jaw-associated prey acquisition behaviours.

The level of stereotypy in raking MAPs

Overall, muscle activity total duration varied much less during raking than during strikes in *O. mykiss*, whereas mean rake durations for both species fell within a surprisingly consistent interval of 150–160±31 ms. In the multivariate analysis there was remarkably little variation in rake MAPs among *O. mykiss* individuals (Fig. 4B), whereas the scatter of rake EMGs across PC axes 1 and 2 was more pronounced in *S. jardinii* (Fig. 5). However, pronounced variation in *O. mykiss* strikes relative to other behaviours (Fig. 4) corresponds well with this taxon utilising a generalist prey-capture behaviour (Liem, 1980).

Clearly, a high degree of behavioural stereotypy governs raking in *O. mykiss*, either because of architectural properties of the cleithrobranchial ligament, or, as suggested by the highly conservative temporal MAPs, resulting from a more tightly controlled central oscillator mechanism than in *S. jardinii*. The mechanisms facilitating and regulating stereotypy in basal vertebrates remain unknown, as fusimotor feedback loops have not been demonstrated (Ross et al., 2007). Still, the identification of proto-muscle spindles in a salmonid jaw adductor muscle (Maeda et al., 1978) suggests an evolutionary origin of neuromotor control governing stereotypical prey-processing mechanisms among pre-tetrapodean gnathostomes. The restricted raking MAP spread, and clear lack of recruitment differences suggests that the functional basis of this behaviour somehow lacks the prerequisites for modulation. It may also be that inter-specific differences exist in the central neural oscillators controlling raking MAPs, which would explain the rake-specific convergence in MAP timing traits (see below). Indeed, raking kinematics in the salmonid *Salvelinus fontinalis* were devoid of modulation in response to biomechanical prey-type differences (Sanford, 2001b), whereas a kinematic prey-type effect in response to comparable prey types was detected in the basal osteoglossomorph *Chitala* (Sanford and Lauder, 1990). Without investigation of additional taxa it remains unknown whether raking modulation is the ancestral or derived condition. One promising avenue for future work will be to ascertain if MAP stereotypy, or lack thereof, is linked to modulation in derived taxa.

Is raking governed by a convergently derived muscle-activity pattern?

Electromyography data from raking in *O. mykiss* and *S. jardinii* provide strong evidence that a convergently derived MAP is governing raking in these evolutionarily distinct lineages. The close apposition of raking MAPs in the principal component plots, relative to alternative feeding behaviours in both taxa (Fig. 6), is driven by a 100% consistent convergence in early AM and PH activity-onset timing, being the principal factors discriminating raking MAPs from strike and chew MAPs overall (Fig. 3). Although the resulting MAP is a novelty in motor-pattern research, these convergent variables primarily govern the raking preparatory phase. Raking MAPs displayed onset-timing sequences (PH>AM>EP>SH>HP) with consistency indices of 73% (*O. mykiss*; $N=106$ rakes) and 75% (*S. jardinii*; $N=130$ rakes). The remaining onset timing sequence only differed for the SH, HP and EP between species. A proportion of this variation, at least in *S. jardinii*, could be explained by very low raking activity levels in SH and HP (Fig. 3).

Several other lines of evidence support the notion of a convergently derived raking MAP, at the organisational levels of cranial morphology, muscle activity and kinematics. Firstly, the morphological key criteria for a TBA are presence of a cleithrobranchial ligament and derived basihyal dentition, none of

which are present in basal teleosts (Sanford and Lauder, 1989), or in the basal salmonid taxa *Coregonus* and *Thymallus* (C.P.J.S., personal observation). Although fish oral cavities commonly are adorned with dermal teeth, basal teleosts, such as *Amia*, *Lepisosteus* and *Polypterus* do not possess basihyal fangs with opposing vomerine or parasphenoid tooth plates, nor do they have a CBL (Sanford and Lauder, 1989). Secondly, previously presented muscle-activity data for these basal taxa provided no evidence of early activity onset in the jaw adductor and basihyal protractor musculature, either during prey capture, or during intra-oral prey processing (chewing and prey transport) (Lauder, 1980; Sanford and Lauder, 1989). Thirdly, every other described feeding behaviour involving the oral jaw apparatus is characterized by a pronounced *expansive phase* involving mandible abduction. By contrast, raking is a unique feeding behaviour that involves early and maintained strong oral jaw adduction throughout the behaviour.

It is commonly assumed that convergent morphologies that face similar functional demands are generally associated with convergent motor-activity patterns (MAPs); however, there has been no documented evidence of this. Indeed, Sanford (Sanford, 2001a) presented kinematic evidence that would seem to contradict this assertion in the TBA of two closely related notopterid knifefishes. Thus, our finding of convergently derived raking MAPs in representatives of two different teleostean lineages suggests that MAPs, even in coupled systems, are labile and have not posed a limitation in the origin and diversification of novel feeding behaviours. Nevertheless, our findings further suggest that once a novel MAP is established it can be highly stereotypical.

Conclusion

The MAPs of five cranial muscles differed markedly between raking, and the strike and chewing behaviours in *O. mykiss*, whereas inter-specific comparisons of raking MAPs between *O. mykiss* and *S. jardinii* revealed more subtle, albeit significant, differences. In both taxa, intraspecific MAP variability was much less during raking than other behaviours. Early activity onset in PH and AM musculature, driving basihyal protraction and lower jaw occlusion, respectively, are convergently derived traits, only found in raking MAPs. This is strong evidence of a convergently derived motor pattern driving raking in at least these taxon representatives from evolutionarily unrelated lineages. However, both muscles exert their primary role during the raking preparatory phase, whereas the ‘power-stroke’ muscles exhibit more labile onset-timing patterns during raking.

LIST OF ABBREVIATIONS

AM	adductor mandibularis
CBL	cleithrobranchial ligament
EMG	electromyography
EP	epaxialis
HL	head length
HP	hypaxialis
MAP	muscle-activity pattern
PH	protractor hyoideus
PIM	posterior intermandibularis
SH	sternohyoideus
TBA	tongue-bite apparatus
TL	total length

Thanks to Cold Spring Harbour Fish Hatchery for sourcing specimens, to M. Ajemian, M. McGuire, P. Wiehl, M. Kats, S. Watts and R. Bershader for help with experiments, to the Hofstra University Animal Care Facility staff for specimen maintenance, and to P. Doherty, A. Camp and two anonymous reviewers for comments that greatly improved the manuscript quality. This work was funded by the National Science Foundation (IOB#0444891, DBI#0420440).

REFERENCES

- Alfaro, M. E. and Herrel, A. (2001). Introduction: major issues of feeding motor control in vertebrates. *Am. Zool.* **41**, 1243-1247.
- Alfaro, M. E. and Westneat, M. W. (1999). Motor patterns of herbivorous feeding: electromyographic analysis of biting in the parrotfishes *Cetoscarus bicolor* and *Scarus iseri*. *Brain Behav. Evol.* **54**, 205-222.
- Alfaro, M. E., Janowetz, J. and Westneat, M. W. (2001). Motor control across trophic strategies: muscle activity of biting and suction feeding fishes. *Am. Zool.* **41**, 1266-1279.
- Carroll, A. M. (2004). Muscle activation and strain during suction feeding in the largemouth bass, *Micropterus salmoides*. *J. Exp. Biol.* **207**, 983-991.
- Carroll, A. M. and Wainwright, P. C. (2006). Muscle function and power output during suction feeding in largemouth bass, *Micropterus salmoides*. *Comp. Biochem. Physiol.* **143A**, 389-399.
- Carroll, A. M., Wainwright, P. C., Huskey, S. H., Collar, D. C. and Turingan, R. G. (2004). Morphology predicts suction feeding performance in centrarchid fishes. *J. Exp. Biol.* **207**, 3873-3881.
- Friel, J. P. and Wainwright, P. C. (1997). A model system of structural duplication: homologies of adductor mandibularis muscles in Tetraodontiform fishes. *Syst. Biol.* **46**, 441-463.
- Friel, J. P. and Wainwright, P. C. (1998). Evolution of motor patterns in tetraodontiform fishes: does muscle duplication lead to functional diversification? *Brain Behav. Evol.* **52**, 159-170.
- Frost, B. J. and Sanford, C. P. J. (1999). Kinematics of a novel feeding mechanism in the osteoglossomorph fish *Chitala chitala*: is there a prey-type effect? *Zoology* **102**, 18-30.
- Greenwood, P. H. and Lauder, G. V. (1981). The protractor pectoralis muscle and the classification of teleost fishes. *Bull. Br. Mus. Nat. Hist. Zool.* **41**, 213-234.
- Grubich, J. R. (2001). Prey capture in actinopterygian fishes: a review of suction feeding motor patterns with new evidence from an elopomorph fish, *Megalops atlanticus*. *Am. Zool.* **41**, 1258-1265.
- Grubich, J. R. and Wainwright, P. C. (1997). Motor basis of feeding performance in largemouth bass (*Micropterus salmoides*). *J. Exp. Zool.* **277**, 1-13.
- Grubich, J. R. and Westneat, M. W. (2006). Four-bar linkage modelling in teleost pharyngeal jaws: computer simulations of bite kinetics. *J. Anat.* **209**, 79-92.
- Hilton, E. J. (2001). Tongue bite apparatus of osteoglossomorph fishes: variation of a character complex. *Copeia* **2001**, 372-381.
- Hilton, E. J. (2003). Comparative osteology and phylogenetic systematics of fossil and living bony-tongue fishes (Actinopterygii, Teleostei; Osteoglossomorpha). *Zool. J. Linn. Soc.* **137**, 1-100.
- Lauder, G. V. (1980). Evolution of the feeding mechanism in primitive actinopterygian fishes: a functional anatomical analysis of *Polypterus*, *Lepisosteus*, and *Amia*. *J. Morphol.* **163**, 283-317.
- Lauder, G. V. (1981). Intraspecific functional repertoires in the feeding mechanism of the characid fishes *Lebiasina*, *Hoplias* and *Chalceus*. *Copeia* **1981**, 154-168.
- Lauder, G. V. (1985). Aquatic feeding in lower vertebrates. In *Functional Vertebrate Morphology* (ed. M. Hildebrand, D. M. Bramble, K. F. Liem and D. B. Wake), pp. 210-229. Cambridge, MA, London: The Belknap Press, Harvard University Press.
- Lauder, G. V. and Liem, K. F. (1983). The evolution and interrelationships of the Actinopterygian fishes. *Bull. Mus. Comp. Zool. Harvard* **150**, 95-197.
- Lauder, G. V. and Reilly, S. M. (1994). Amphibian feeding behavior: comparative biomechanics and evolution. In *Biomechanics of Feeding in Vertebrates: Advances in Comparative and Environmental Physiology*. Vol. 18 (ed. V. Bels, M. Chardon and P. Vandewalle), pp. 163-195. Berlin: Springer-Verlag.
- Liem, K. F. (1970). Comparative functional anatomy of the Nandidae (Pisces: Teleostei). *Fieldiana Zool.* **56**, 1-166.
- Liem, K. F. (1978). Modulatory multiplicity in the functional repertoire of the feeding mechanism in cichlid fishes. I. Piscivores. *J. Morphol.* **158**, 323-360.
- Liem, K. F. (1980). Adaptive significance of intra- and interspecific differences in the feeding repertoires of cichlid fishes. *Am. Zool.* **20**, 295-314.
- Maeda, N., Miyoshi, S. and Toh, H. (1978). First observation of a muscle spindle in fish. *Nature* **302**, 61-62.
- Motta, P. J., Tricas, T. C., Hueter, R. E. and Summers, A. P. (1997). Feeding mechanism and functional morphology of the jaws of the lemon shark *Negaprion brevirostris* (Chondrichthyes, Carcharhinidae). *J. Exp. Biol.* **200**, 2765-2780.
- Munday, P. L. and Wilson, S. K. (1997). Comparative efficacy of clove oil and other chemicals in anaesthetization of *Pomacentrus amboinensis*, a coral reef fish. *J. Fish Biol.* **51**, 931-938.
- Ojanguren, A. F. and Brana, F. (2000). Thermal dependence of swimming endurance in juvenile brown trout. *J. Fish Biol.* **56**, 1342-1347.
- Reilly, S. M. (1995). The ontogeny of aquatic feeding behavior in *Salamandra salamandra*: stereotypy and isometry in feeding kinematics. *J. Exp. Biol.* **198**, 701-708.
- Ross, C. F., Eckhardt, A., Herrel, A., Hylander, W. L., Metzger, K. A., Schaeferlaeken, V., Washington, R. L. and Williams, S. H. (2008). Modulation of intra-oral processing in mammals and lepidosaurs. *Integr. Comp. Biol.* **47**, 118-136.
- Sanford, C. P. J. (2001a). The novel 'tongue-bite apparatus' in the knife-fish family Notopteridae (Teleostei: Osteoglossomorpha): are kinematic patterns conserved within a clade? *Zool. J. Linn. Soc.* **132**, 259-275.
- Sanford, C. P. J. (2001b). Kinematic analysis of a novel feeding mechanism in the brook trout *Salvelinus fontinalis* (Teleostei: Salmonidae): behavioural modulation of a functional novelty. *J. Exp. Biol.* **204**, 3905-3916.
- Sanford, C. P. J. and Lauder, G. V. (1989). Functional morphology of the "Tongue-Bite" in the Osteoglossomorph fish *Notopterus*. *J. Morphol.* **202**, 379-408.
- Sanford, C. P. J. and Lauder, G. V. (1990). Kinematics of the tongue-bite apparatus in osteoglossomorph fishes. *J. Exp. Biol.* **154**, 137-162.
- Shaffer, H. B. and Lauder, G. V. (1985). Aquatic prey capture in ambystomatid salamanders: patterns of variation in muscle activity. *J. Morphol.* **183**, 273-284.
- Sibbing, F. A., Osse, J. W. M. and Terlouw, A. (1986). Food handling in the carp (*Cyprinus carpio*): its movement patterns, mechanisms, and limitations. *J. Zool. Lond.* **210**, 161-203.
- Van Wassenbergh, S., Herrel, A., Adriaens, D. and Aerts, P. (2005). A test of mouth-opening and hyoid-depression mechanisms during prey capture in a catfish. *J. Exp. Biol.* **208**, 4627-4639.
- Van Wassenbergh, S., Herrel, A., Adriaens, D. and Aerts, P. (2006). Modulation and variability of prey capture kinematics in clariid catfishes. *J. Exp. Zool. A* **305**, 559-569.
- Van Wassenbergh, S., Herrel, A., Adriaens, D. and Aerts, P. (2007a). Interspecific variation in sternohyoideus muscle morphology in clariid catfishes: functional implications for suction feeding. *J. Morphol.* **268**, 232-242.
- Van Wassenbergh, S., Herrel, A., Adriaens, D. and Aerts, P. (2007b). No trade-off between biting and suction feeding performance in clariid catfishes. *J. Exp. Biol.* **210**, 27-36.
- Van Wassenbergh, S., Herrel, A., James, R. S. and Aerts, P. (2007c). Scaling of contractile properties of catfish feeding muscles. *J. Exp. Biol.* **210**, 1183-1193.
- Wainwright, P. C. and Turingan, R. G. (1993). Coupled vs uncoupled functional systems: motor plasticity in the queen triggerfish, *Balistes vetula* (Teleostei, Ballistidae). *J. Exp. Biol.* **180**, 209-227.
- Wainwright, P. C. (1989a). Functional morphology of the pharyngeal jaws in perciform fishes: an experimental analysis of the Haemulidae. *J. Morphol.* **200**, 231-245.
- Wainwright, P. C. (1989b). Prey processing in haemulid fishes: patterns of variation in pharyngeal jaw muscle activity. *J. Exp. Biol.* **141**, 359-376.
- Wainwright, P. C. (2002). The evolution of feeding motor patterns in vertebrates. *Curr. Opin. Neurobiol.* **12**, 691-695.
- Wainwright, P. C. (2005). Functional morphology of the pharyngeal jaw apparatus. In *Biomechanics of Fishes* (ed. R. Shadwick and G. V. Lauder), pp. 77-101. San Diego: Academic Press.
- Wainwright, P. C. and Friel, J. P. (2000). Effects of prey type on motor pattern variance in tetraodontiform fishes. *J. Exp. Zool.* **286**, 563-571.
- Wainwright, P. C. and Friel, J. P. (2001). Behavioral characters and historical properties of motor patterns. In *The Character Concept* (ed. G. Wagner), pp. 285-301. San Diego: Academic Press.
- Wainwright, P. C., Sanford, C. P., Reilly, S. M. and Lauder, G. V. (1989). Evolution of motor patterns: aquatic feeding in salamanders and ray-finned fishes. *Brain Behav. Evol.* **34**, 324-341.
- Zar, J. H. (1999). *Biostatistical Analysis* (4th edn). New Jersey: Prentice Hall.